

Dedicated to Acad. Prof. Dr. Margareta Giurgea with the occasion of her 90-th anniversary

## **SURFACE ENHANCED RAMAN SCATTERING AND PHOTOLUMINESCENCE STUDIES ON SINGLE-WALLED CARBON NANOTUBES SUBMITTED TO NON-HYDROSTATIC COMPRESSION**

M. Baibarac, I. Baltog<sup>\*</sup>, L. Mihut, N. Preda, T. Velula, C. Godon<sup>a</sup>, J. Y. Mevellec<sup>a</sup>, J. Wéry<sup>a</sup>, S. Lefrant<sup>a</sup>

National Institute of Materials, Lab. of Optics and Spectroscopy, P. O. Box MG-7, RO-77125, Bucharest, Romania

<sup>a</sup>Institut de Materiaux de Nantes, Laboratoire de Physique Cristalline, 2 Rue de la Houssiniere, B.P. 32229, 44322 Nantes, France

Single-walled carbon nanotubes (SWNTs) under a moderate non-hydrostatic pressure, of 0.58 GPa, undergo a non-reversible transformation. Due to the plastic deformations, structural defects and carbon nanotube fragments of different size are produced. Short fragments of spherical or ellipsoidal form, behaving as closed-shell fullerenes are observed both by Raman spectroscopy and photoluminescence (PL). The main vibrational indicative of the fragments of shorter length is the band at  $\sim 1458 \text{ cm}^{-1}$  that is regularly observed in the Raman spectra of fullerene. Similar to fullerenes self assemblies, the interaction between the nanotube fragments is noticed in the Raman spectrum by the band at  $\sim 94 \text{ cm}^{-1}$  that reveals an inter-particle vibration mode. When the nanotubes are dispersed into host matrix, as aromatic hydrocarbons (AHs) with isolated or condensed phenyl rings, supplementary mechanico-chemical reactions take place. For AHs with isolated phenyl rings, like biphenyl or p-terphenyl, a chemical functionalization of SWNT fragments is demonstrated by the appearance of a new Raman band at  $1160 \text{ cm}^{-1}$ . In PL spectra, the interaction of SWNTs with AHs, is noticed by a detailed vibronic structure appearing in the high energy side of the emission spectrum, that increase with the weight of SWNTs in the AHs/SWNTs mixtures.

(Received July 4, 2005; accepted July 21, 2005)

*Keywords:* Carbon nanotubes, Non-hydrostatic compression, Aromatic hydrocarbons, Raman spectroscopy, Photoluminescence

### **1. Introduction**

Single-walled carbon nanotubes (SWNTs) represent a basic compound in the generation of new advanced materials. The great interest for “the tubes manipulation” during composite synthesis explains the considerable effort devoted to covalent, non-covalent and/or ionic functionalization of SWNTs as a method of their solubilization in different solvents [1]. Physical properties of composites depend on the preparation method. An example is the polyaniline/SWNTs composite, which exhibits different vibrational properties when is prepared by the direct mixing of the two compounds or by chemical polymerization of aniline in the presence of SWNTs [2]. The difference originates in the reaction between SWNTs and the polymerization medium [3]. In the polyaniline/SWNTs composites, the small tube fragments are recognized in the final product by fullerene like phonon signatures [2]. Other ways of SWNT transformation are ball milling [4] and mechanico-chemical process [5]. A solid-phase mechanico-chemical reaction between SWNTs and KOH has been recently reported [6]. In this paper, such a mechanico-chemical reaction is achieved by a non-hydrostatic compression of SWNTs which were previously dispersed into various aromatic host matrix. Generally, such a transformation may produce large changes in the electronical, optical

---

\* Corresponding author: ibaltog@infim.ro

and structure properties of the compressed solids [7]. Raman spectroscopy is a suitable method to put it in evidence changes induce in the phonon spectrum. The investigation of isolated tubes confronts with the difficulty to measure very weak Raman signals that is overtaken using the surface-enhanced Raman scattering (SERS) which operates with enhanced Raman signals due to the resonant excitation of surface plasmons [8].

Using SERS and photoluminescence (PL) spectroscopy and transmission electron microscopy (TEM), we show that SWNTs non-hydrostatically compressed at 0.58 GPa break in fragments of different sizes, some displaying a phonon spectrum like fullerene. The neutral and charged SWNTs fragments (behaving as cation and anion radicals) result from a homolytically and heterolytically breaking of carbon-carbon covalent bonds, respectively. We show that dispersing SWNTs in different host matrices one induces mechanico-chemical reactions which result in the functionalization of nanotubes and its fragments.

## 2. Experimental

SWNTs were produced by the electric arc technique [9]. Nanotubes, alone or dispersed into aromatic host matrices as biphenyl, naphthalene, p-terphenyl and phenanthrene were compressed 5 minutes at 0.58 GPa. High pressure was generated in a steel-anvil. The samples in form of pellets of 12 mm diameter and 0.1 mm thickness were confined in the space between two steel disks. For SERS measurements the pellets were ultrasonically dispersed in toluene. Films of 150 nm thickness were prepared by evaporation of toluene from a "solution" of known concentration, spread on the rough Au substrates. SERS studies were performed in a backscattering geometry, under laser excitation wavelengths 1064 and 676.4 nm, using a RFS 100 FT Raman Bruker spectrophotometer and a Jobin Yvon T64000 Raman-spectrophotometer, respectively. PL spectra were obtained in a right angle geometry using a Jobin Yvon Fluorolog-3 spectrometer. Transmission electron microscopy (TEM) images of compressed tubes alone or dispersed in different matrices were recorded with a HF 2000 Hitachi microscope operating at 200 KV.

## 3. Results and discussion

The SERS spectra on uncompressed SWNT films at 1064 nm and 676.44 nm excitation wavelengths are presented in Fig. 1 a<sub>1</sub> and a<sub>2</sub>, respectively. Two Raman spectral ranges are of interest 50 – 250 and 1100 – 1700 cm<sup>-1</sup>. In the former interval, one finds bands associated to radial breathing modes (RBM) [10] whose peak position is sensitive to the excitation wavelength. Radial bands at 164 and 174 cm<sup>-1</sup>, under 1064 and 676.4 nm excitations, indicate a resonance effect occurring over a narrow range of diameters around 1.35 – 1.30 nm, identified with transitions between the Van Hove singularities E<sub>22</sub><sup>S</sup> and E<sub>11</sub><sup>M</sup> in the valence and conduction bands of semiconducting and metallic tubes, respectively [11]. In the range 1100 – 1700 cm<sup>-1</sup>, the bands, labeled G and D, are displayed with changes in frequency, line-shape and intensity under various excitations. The former, with a maximum at 1595 cm<sup>-1</sup> attributed to in-plane stretching E<sub>2g</sub> vibration (tangential mode – TM), is also present in the Raman spectrum of other graphitic materials, like highly oriented pyrolytic graphite (HOPG), glassy carbon, etc. [10]. A specific signature of the metallic tubes is found under a laser excitation energy between 1.5 – 2.2 eV. For λ<sub>exc.</sub> = 676.4 nm, it consists in a wide TM band with an asymmetric profile of Breit-Wigner-Fano (BWF) type, peaking around 1540 cm<sup>-1</sup>, which originates from electron-phonon interactions [12]. D band, found both in SWNTs and graphite lattices, has a peak position that depends on the excitation energy and its growth in intensity indicates disorder or defects induced in SWNTs structure [10].

Figs. 1b show the modification of phonon spectrum of the SWNTs submitted to a non-hydrostatic compression at 0.58 GPa. The Raman spectra indicate the formation of tube fragments which interact between them. By breaking, free radicals and/or anion and cation radicals are formed, which later on results in neutral and charged SWNT fragments, respectively. When SWNTs are compressed alone or dispersed into non-reactive host matrix, a homolytical breaking is expected to takes place. Generally, the free radicals are unstable and tend to mend the initial bond quickly. The

final result consists in the formation of SWNT fragments of different size. The larger fragments behave like nanotubes preserving greatly the basic properties of the SWNTs. The fact that in Figs. 1b, the BWF component is still observed indicates that only a partial destroying of metallic tubes taken place. The enhancement of the D band evidences an increased state of disorder and defects achieved by the nanotube breaking. The shorter fragments, of ellipsoidal/spherical form, behaving as closed-shell fullerene precursors, are spotted by a weak Raman band around  $1450\text{ cm}^{-1}$  that in  $\text{C}_{60}$  is attributed to  $\text{A}_g(2)$  pentagonal pinch vibration mode (Figs. 1b<sub>1</sub>). Under compression, the SWNT fragments may interact between them and the interaction will be stronger when the formed fragments there are less dispersed. Such a situation one find when the SWNTs are compressed alone. Such an interactions can be looked by analogy with those reported on self-assembled fullerenes which in phonon spectrum are noticed by an asymmetry and a downshift of the  $\text{A}_g(2)$  band and a decrease until disappearance of the Raman bands associated to the radial vibration modes  $\text{A}_g(1)$  and  $\text{H}_g(1)$  [13].

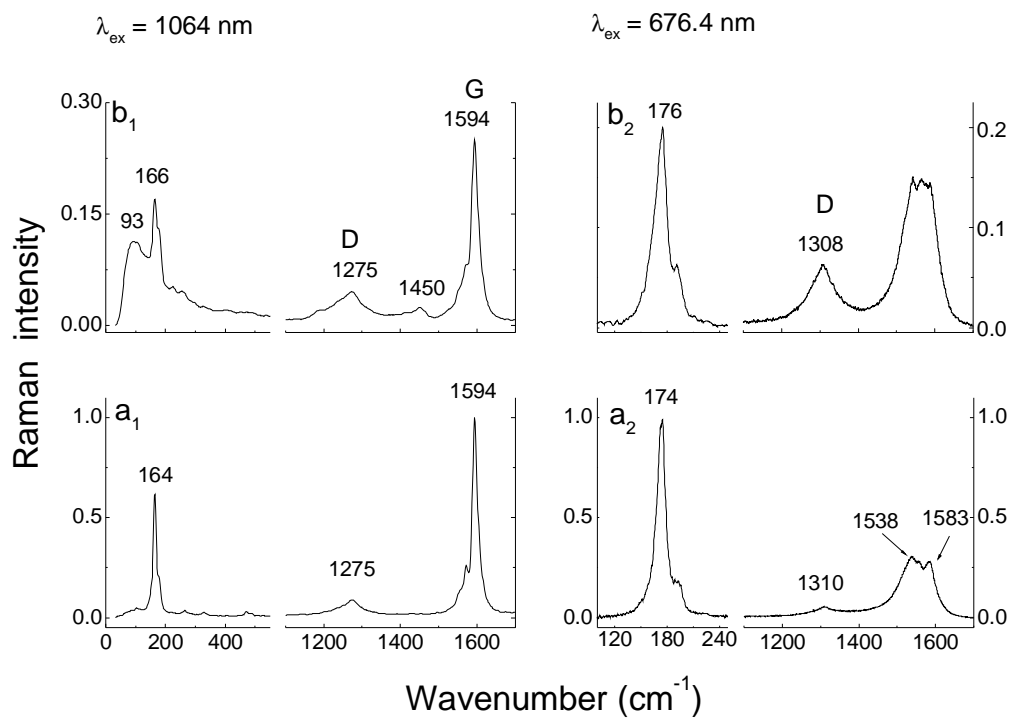


Fig. 1. SERS spectra of SWNTs at two excitation wavelengths before (a) and after their non-hydrostatic compression at 0.58GPa alone (b) and dispersed in  $\text{SiO}_2$  (c).

Besides, a new band at  $94\text{ cm}^{-1}$  [13] that is also observed in  $\text{C}_{120}$  [14] features the self-assembled fullerenes. In this context, the appearance in the SERS spectrum (Figs. 1b<sub>1</sub>, 1c<sub>1</sub>) of a broad band at  $93\text{ cm}^{-1}$ , equally observed on Ag and Au SERS substrates, is significant. It originates in the interactions between the formed SWNTs fragments. TEM images of initial and compressed SWNTs are shown in Fig. 2. The interaction strength depends on the distance between the tube fragments and it can be varied if one disperses the tubes into a host matrices.

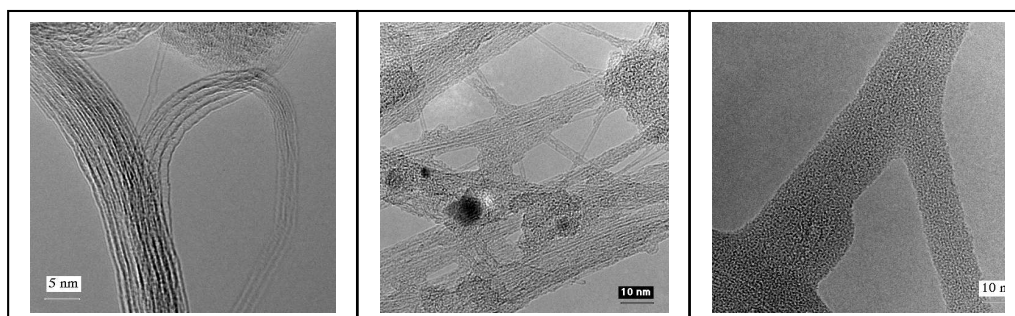


Fig. 2. TEM micrographs of SWNTs after their non-hydrostatic compression at 0.58GPa. From left to right , SWNTs initial, compressed alone and dispersed in p-terphenyl.

If the host matrix has a certain chemical reactivity against SWNTs, an additional chemical transformation may be also observed. Such a different transformation occurs when SWNTs are compressed in aromatic hydrocarbons (AHs) with isolated (biphenyl, p-terphenyl) and condensed (naphthalene, phenantrene) phenyl rings. Regardless of AHs matrix used, the increase of D band intensity is a common feature of the SERS spectra recorded at  $\lambda_{exc.} = 676.4$  nm (Fig. 3).

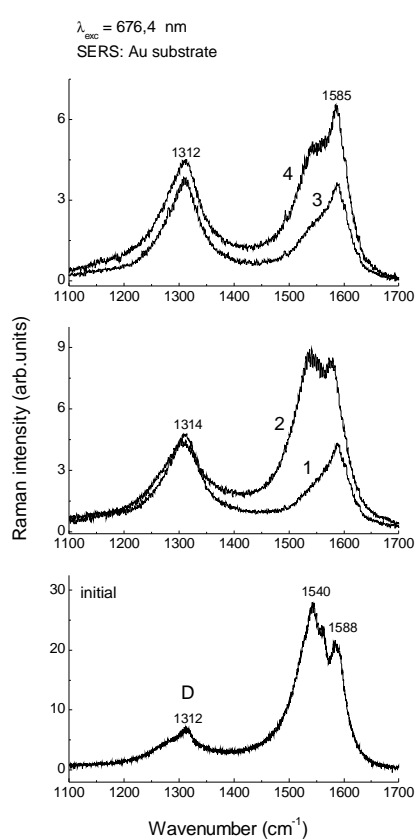


Fig. 3. SERS spectra of SWNTs before (a) and after their compression at 0.58 GPa in biphenyl (1), naphthalene (2), p-terphenyl (3) and phenantrene (4).

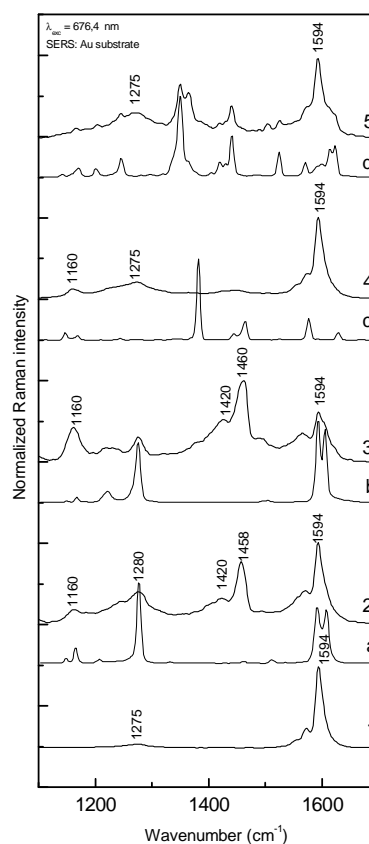


Fig. 4. SERS evidence of the mechano-chemical interaction of SWNTs (1) with biphenyl (2), p-terphenyl (3), naphthalene (4) and phenantrene (5). Curves (a)-(d) correspond to the Raman spectra recorded on powder of biphenyl, p-terphenyl, naphthalene and phenantrene, respectively.

The Raman spectrum ranging between 1400 and 1700  $\text{cm}^{-1}$  (Fig. 3) display a dependence of the type of AHs used as host matrix: i) in naphthalene and phenantrene one obtained 3 - 4 times less intense spectra, displaying a BWF profile no more modified in comparison with that recorded on un-compressed tubes; ii) contrary, in biphenyl and p-terphenyl, a prominent decrease of the BWF component (spectra 1 and 3) takes place. These data show that the two type AHs react differently with SWNTs. Knowing that AHs interact strongly with the basal plane of graphitic surfaces, via  $\pi$ -stacking, a similar interaction can be supposed with the side-walls of SWNTs [15]. In this way a non-covalent functionalization of SWNTs with AHs takes place that preserves the  $\text{sp}^2$  hybridization of carbon atoms maintaining their electronic properties, implicitly the metallic character. Above data suggest that SWNTs compressed in biphenyl and p-terphenyl are covalent and/or ionic functionalized, too. This occurs as a consequence of the biphenyl and p-terphenyl properties to be n/p doped [16] and to react with other AHs as naphthalene [16, 17]. In the latter case may results two compounds: one having formed additional pentagonal rings [16] and another appearing as a biphenyl-doped naphthalene [17]. In this way one explains the appearance of the Raman band, around 1455  $\text{cm}^{-1}$  (curves 2 and 3 in Fig. 4), as signature of the pentagonal rings ( $A_g(2)$  mode) that are formed by the compression of SWNTs in biphenyl or p-terphenyl matrix. This proves that additional pentagonal rings are formed as result of the side-wall covalent functionalization of SWNT fragments. It is worth to notice that the same Raman band at  $\sim 1455 \text{ cm}^{-1}$  has been reported recently on a true p-terphenyl/SWNTs composite [18]. Besides, such an explanation is sustained also by the appearance of a broad Raman line at 1160  $\text{cm}^{-1}$  (spectra 2 and 3, Fig. 4) which in fact contains two components at 1146 and 1174  $\text{cm}^{-1}$  associated with C-H bending vibration modes of the aromatic and quinoid ring of biphenyl or p-terphenyl in un-doped and doped state, respectively [19]. The presence of this band in Fig. 4 indicates the formation of donor-acceptor complexes of the type biphenyl or p-terphenyl doped CNT fragments. The decoration of the side-walls of SWNTs with p-terphenyl is demonstrated by TEM micrographs in Fig. 2c. The clear image from the Fig. 2a of the isolated and bundled tubes practically disappears when biphenyl or p-terphenyl (Fig. 2c) was used as compressing host matrix.

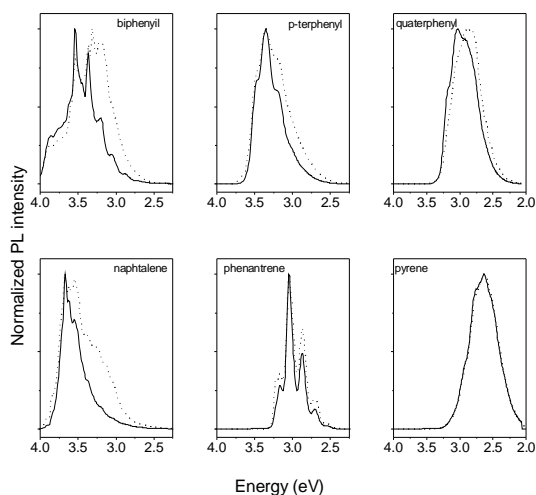


Fig. 5. Photoluminescence at RT of different aromatic hydrocarbons as powder (solid line) and compressed platelet at 0.58 GPa (dotted line).  $\lambda_{\text{exc}} = 265 \text{ nm}$ .

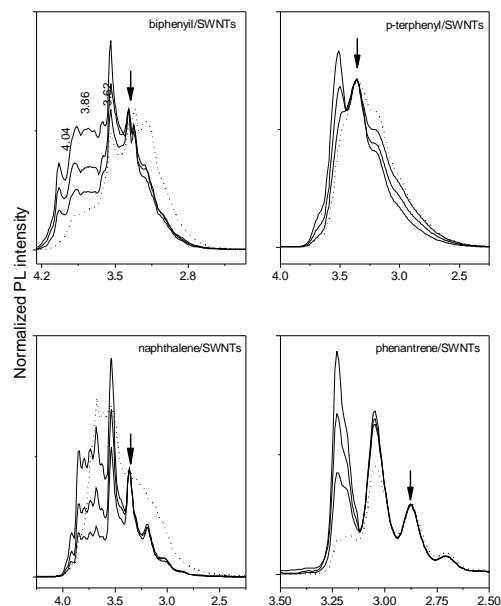


Fig. 6. Photoluminescence at RT of platelets formed by the compression at 0.58 GPa of different mixtures of AHs/SWNTs. The curves from bottom to top illustrate the effect due to the increase of the SWNTs concentration and the dotted line is for the platelet of neat AHs. The SWNTs concentration was: in biphenyl (0; 1; 3; 5 % wt), naphthalene (0; 0.5; 1; 5 % wt), p-terphenyl (0; 0.5; 1; 3 % wt) and phenantrene (0; 0.05; 0.1; 1 % wt). -  $\lambda_{\text{exc}} = 265 \text{ nm}$ . All curves were normalized at the intensity of the  $S_1 \rightarrow S_0/0 \rightarrow 1$  band indicated by an arrow.

An evaluation of the modification of PL spectra of AHs/SWNTs mixture compressed non-hydrostatically must be done in comparison with the behavior of the neat host material. Fully illustrative for this, is Fig. 5. As first finding we notice that no great difference in the magnitude of the global PL emission was observed when the measurements were done on powder or compressed platelet. The two curves, solid and dotted, show the PL spectra on grinded powder containing particle of micronic size and the platelet provided by compression at 0.58 GPa, respectively. The broadening of the emission spectrum in the low energy side is the most significant result. It is similar with other reported data concerning the high-pressure effect on the luminescence of AHs [20-22].

As consequence of the compression, the intermolecular interactions become stronger and shift the electronic transitions toward lower energies although the integrated intensity remains approximately constant. Another contribution to the wide PL profile can originate in an excimeric emission. As results of the strong mechanical package an electronic overlap is produced and the probability that a molecule excited to form excimers with its neighbors is much increased. The excimers are molecular complexes definite by different binding energy in the excited state. These features of the PL spectra of compressed neat AHs are not more observed in the mixture with SWNTs. In comparison with the platelets prepared from the neat AHs, a general feature of compressed AHs/SWNTs mixtures is a much weaker global PL emission. The increase of the nanotubes weight in the AHs/SWNTs mixtures induces a quenching process of the luminescence. We note that the modification by compression of the PL emission is not the same for different AHs, it depends on how many phenyl rings are bound together and if the AHs molecule contains isolated or fused phenyl rings. Thus, the compression effect on the PL emission is greater both in the case of AHs of smaller size molecules (i.e. biphenyl and naphthalene) and AHs with isolated phenyl rings (i.e. biphenyl and p-terphenyl). Contrary to the variation induced by hydrostatic compression in PL spectrum of AHs, which is reversible in the greatest part, it disappearing with the ceasing of high pressure, in the present case we notice as typical effect of non-hydrostatic compression the persistence for longer time of the modified PL emission. Besides, by the increase of the nanotubes weight in the AHs/SWNTs mixtures, the PL spectra display a more and more detailed vibronic structure straightening in the high energy side. These variations of PL spectra represent the signature of functionalization of the SWNTs or nanotube fragments with AHs molecules. In this frame, when the AHs molecule plays the roll of luminescence cite in the AHs/SWNTs composite one can suppose that in the generation of PL emission there are two contributions: one that is due to intramolecular transitions (pure electronic and vibronic) that takes place in the AHs molecule and another that reflects coupling of these transitions to the intermolecular vibrations (phonons) field of the environment. In the latter case one must named the interactions between nanotubes, nanotubes fragments and AHs molecules. The former contribution gives rise to Lorentzian-shaped zero-phonon lines, with widths determined by the de-phasing times of the excited state while the latter lead to the changes of the phonon spectrum as rule observed in the low frequencies range of the Raman spectra. Generally, in AHs molecules, the smaller coupling of the C-C vibrations to the electronic transition emphasizes the  $S_1 \rightarrow S_0/0 \rightarrow 0$  transition in both absorption and fluorescence at the expense of the  $S_1 \rightarrow S_0/0 \rightarrow 1$  and higher transitions [23]. This interdependence determines the shapes of the PL spectra from Fig. 5, where one see that the powder state, less favorable for mutual interactions, is featured by an enhancement of the  $S_1 \rightarrow S_0/0 \rightarrow 0$  band. We used the notation  $S_1 \rightarrow S_0/n \rightarrow m$  that denotes a transition from the first singlet excited state  $S_1$  to the ground state  $S_0$  and between the  $n$ th vibration level of  $S_1$  to  $m$ th vibration level of  $S_0$ . In general, due to a self-absorption process, the phonon wing and zero-phonon line are masked, their observation can be better done at low temperature, when the absorption and emission spectra are more separated. The two contributions to the PL emission of p-terphenyl platelet become observable by measurements at room and liquid nitrogen temperatures (RT; LNT), in Fig. 7a. The main feature of the PL spectrum recorded at LNT is the appearance of a well resolved vibronic progression in steps of  $\sim 0.15$  eV. The most intense band at  $\sim 3.5$  eV is associated to the  $S_1 \rightarrow S_0/0 \rightarrow 0$  transition. At RT, due to the self absorption this band appears as a weak shoulder, the more intense band is that associated to the transition  $S_1 \rightarrow S_0/0 \rightarrow 1$ .

A striking result for the AHs/SWNTs mixture is showed in Fig. 7b. It consisting in almost identical PL spectra at RT and LNT that in turn resembles with the spectrum of neat AHs at LNT. On Fig. 7b we notice the presence of a new band, peaking at 3.68 eV, that enhances constantly with

the increase of SWNTs weight. Its blue shift of about 0.17 eV, not so far of those above mentioned  $\sim 0.15$  eV, suggests a  $S_1 \rightarrow S_0/1 \rightarrow 0$  transition. This is explainable taking into account the strong perturbation produced by the strong environmental phonon field resulted from the interaction between AHs and nanotubes bundled or dispersed as individual units. Thus, an over population of the superior vibronic level of the excited electronic state is produced. It is evident that such a perturbation, resulting from an intermolecular interaction can be observed also on neat compressed AHs, without the addition of nanotubes. In Fig. 7a, the presence of the weak band with maximum at 3.63 eV must be interpreted in this way. The same results were obtained on other systems. An additional vibronic series stepping by  $\sim 0.175$  eV that increases with the content of SWNTs is observed in the blue part of the PL spectrum of biphenyl/SWNTs platelet. For the phenantrene/SWNTs platelets, the roll of SWNTs limits only to a gradual increasing of the  $S_1 \rightarrow S_0/0 \rightarrow 0$  band.

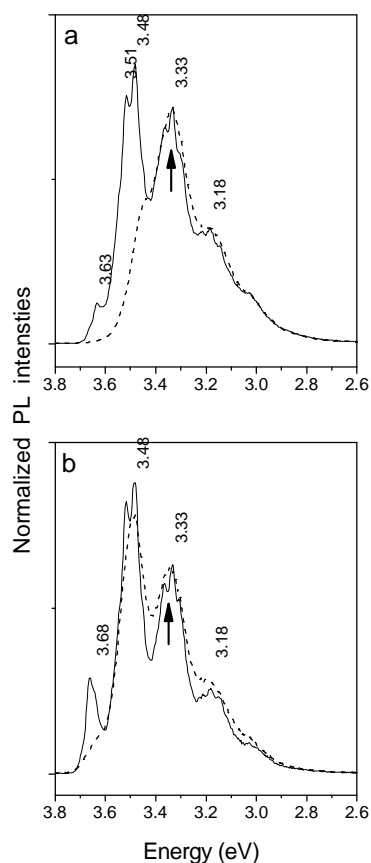


Fig. 7. Photoluminescence at RT (dashed line) and LNT (solid line) of p-terphenyl alone (a) and p-terphenyl /SWNTs (3 % wt) mixture (b) compressed non-hydrostatically at 0.58 GPa.

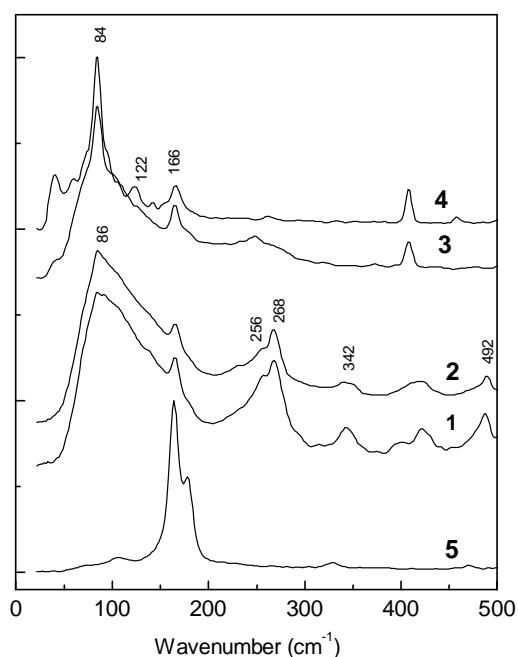


Fig. 8. SERS spectra at  $\lambda_{exc} = 1064$  nm on Au substrate of the SWNTs compressed non-hydrostatically at 0.528 GPa in mixture with biphenyl (1), terphenyl (2), phenantrene (3) and pyrene (4). The spectrum 5 is for uncompressed SWNTs.

Returning to the Raman spectra we remind that on biphenyl/SWNTs and p-terphenyl/SWNTs platelets was observed a supplementary Raman band, around  $1455 \text{ cm}^{-1}$  (curves 2 and 3 in Fig. 4) which was reported in the Raman spectra of  $C_{60}$ , it being associated with as  $A_g(2)$  mode of pentagonal rings. In our case, this band may originates in: i) a pentagonal pinch mode, as an  $A_g(2)$  mode, activated in the nanotube fragments, of small size of spherical or ellipsoidal form, resulting by the breaking of SWNTs and ii) the additional pentagonal rings formed by the interaction of the AHs

molecules having isolated phenyl rings with the side-walls of SWNTs. Taking into account these two contribution, the Raman lines appearing at ca. 256-268 and 492  $\text{cm}^{-1}$  could be regarded as bands associated to the  $H_g(8)$  and  $A_g(1)$  vibration mode, respectively of  $C_{60}$  [10]. We note that the new band at 342  $\text{cm}^{-1}$  is a typical signature in the SERS spectra of the interaction of fullerene like particles with the gold substrate [13].

As in SERS spectra of  $C_{60}$  self-assemblies [24], in Fig. 8 we observe the down shift of the  $H_g(8)$ , its broadening in the low energy side with the formation of a new Raman band at  $\sim 256 \text{ cm}^{-1}$  as well as the appearance of a new and large band at about  $\sim 85 \text{ cm}^{-1}$  [13]. The latter band, not uniquely related to the fullerene like particles, is observed also resulting from the interaction polymer - SWNTs [2]. Such a modification is clear shown in Fig. 9, on the sample prepared from the platelet of biphenyl/ SWNTs and p-terphenyl/SWNTs and no on the samples originating in phenantrene/SWNTs platelet.

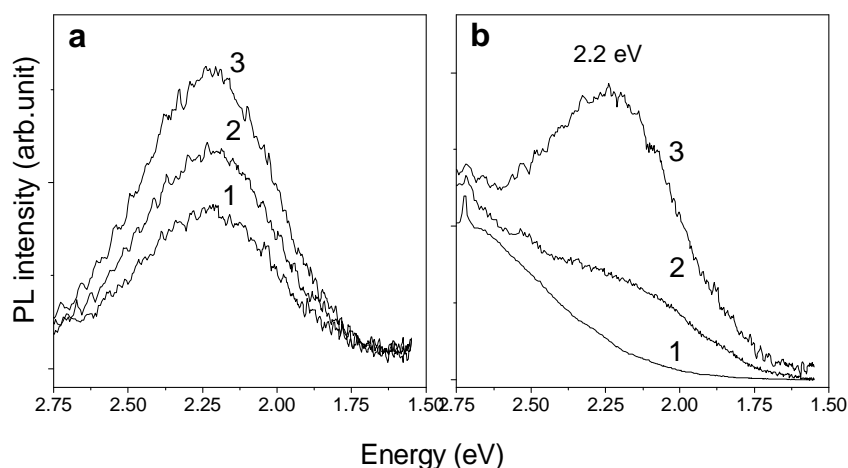


Fig. 9. Photoluminescence at RT of non-hydrostatically compressed platelets, at 0.58 GPa, of SWNTs mixed with biphenyl/SWNTs(a) and p-terphenyl/SWNTs (b). In (a), the curves 1, 2 and 3 were obtained by subtraction and correspond to a SWNTs weight in the compressed mixture of 0.1, 1 and 10 %, respectively. In (b) the curves 1, 2 and 3 show the PL spectra of compressed p-terphenyl alone and mixed with 0.1 and 10 % SWNTs, respectively –  $\lambda_{\text{exc}} = 265 \text{ nm}$ .

A priori, this intensification of the fullerene-like signature should be observed also in the PL spectra. Indeed, in the low energy side of PL spectra of the the biphenyl/SWNTs and p-terphenyl/SWNTs platelets one finds a supplementary emission band at  $\sim 2.24 \text{ eV}$  that not belongs to the AHs PL spectrum. This band, growing with the SWNTs concentration, has the characteristics of the  $C_{60}$  emission after a self-assembling process occurred in reactive solvents as N-methyl-2-pyrrolidinone or pyrrolidine [25]. We note that, in the present case the host matrix of the type biphenyl or p-terphenyl plays the role of the reactive solvent, above mentioned.

#### 4. Conclusions

The main results of this paper are summarized as follows: i) SWNTs compressed, at 0.58 GPa, break in fragments of different sizes. The small fragments, behaving as precursor of fullerenes, are evidenced by Raman bands at 1450 and 93  $\text{cm}^{-1}$ ; ii) using aromatic hydrocarbons as compressing host matrices a non-covalent functionalization of SWNTs is produced. Supplementary, for biphenyl and p-terphenyl, an ionic and covalent functionalization of SWNTs fragments is demonstrated; the increase in the intensity of the D Raman band is an indicative of disorder and defects induces by the non-hydrostatic compression of SWNTs. iii) in comparison with the luminescence of neat AHs, the

interactions between AHs and SWNTs or its fragments results in weakness of the global PL emission. A detailed vibronic structure, straightening in the high energy side of the PL spectrum that increase with the weight of SWNTs is another characteristic of the PL spectra of AHs/SWNTs mixtures.

### Acknowledgments

Samples of SWNTs were provided by the “Groupe de Dynamique des Phases Condensées” of the University of Montpellier II. Work performed in the frame of the Scientific Cooperation between the Laboratory of Crystalline Physics of the Institute of Materials in Nantes and the Laboratory of Optics and Spectroscopy of the National Institute of Materials Physics in Bucharest.

### References

- [1] W. P. Sun, K. Fu, Y. Li, W. Huang, *Acc. Chem. Res.* **35**, 1096 (2002).
- [2] M. Baibarac, I. Baltog, S. Lefrant, J. Y. Mevellec, O. Chauvet, *Chem. Mater.* **15**, 4149 (2003).
- [3] S. Lefrant, I. Baltog, M. Baibarac, J. Y. Mevellec, O. Chauvet, *Carbon* **40**, 2201 (2002).
- [4] Y. B. Li, B. Q. Wei, J. Liang, Q. Yu, D. H. Wu, *Carbon* **37**, 493 (1999).
- [5] K. E. Drexler, *Nanosystems: Molecular Machinery Manufacturing & Computation*, John Wiley & Sons, New York, (1992).
- [6] H. Pan, L. Liu, Z. X. Guo, L. Dai, F. Zhang, D. Zhu, R. Czerw, D. L. Carroll, *Nano Letters* **3**, 29 (2003).
- [7] W. Holzapfel, N. S. Isaacs, Editors, *High-Pressure Techniques in Chemistry and Physics: A Practical approach*, Oxford University Press: Oxford and New York, (1997).
- [8] A. Otto, *Surface Enhanced Raman Scattering*, in *Topics in Applied Physics, Light Scattering in Solids IV*, editors: R. K. Chang, T. E. Furtak, vol. **54**, Springer Verlag Berlin, (1984).
- [9] L. Vaccarini, C. Goze, R. Aznar, V. Micholet, C. Journet, P. Bernier, *Synth. Met.* **103**, 2492 (1999).
- [10] M. S. Dresselhaus, G. Dresselhaus, P. C. Eklund, “*Science of Fullerenes and Carbon Nanotubes*”, Academic Press, New York, (1996).
- [11] S. D. M. Brown, P. Corio, P. Marucci, M. S. Dresselhaus, M. A. Pimenta, K. Kneipp, *Phys. Rev. B* **61**, R5137 (2000).
- [12] M. A. Pimenta, A. Marucci, S. A. Empedocles, M. G. Bawendi, E. B. Hanlon, A. M. Rao, C. Eklund, R. E. Smalley, G. Dresselhaus, M. S. Dresselhaus, *Phys. Rev. B* **58**, R16016 (1998).
- [13] M. Baibarac, L. Mihut, N. Preda, I. Baltog, J. Y. Mevellec, S. Lefrant, *Carbon* **43**, 1 (2005).
- [14] S. Lebedkin, H. Rietschel, G. B. Adams, H. J. Eisler, M. Kappwes, W. Kratschmer, *J. Chem. Phys.* **110**, 11768 (1999).
- [15] E. Katz, *J. Electroanal. Chem.* **365**, 157 (1994).
- [16] B. Schlicke, A. D. Schluter, P. Hauser, J. Heinze, *Angew. Chem. Int. Ed. Engl.* **36**, 1997 (1996).
- [17] G. Clydesdale, R. B. Hammond, K. J. Roberts, *J. Phys. Chem. B* **107**, 4826 (2003).
- [18] E. Gregan, S. M. Keogh, A. Maguire, T. G. Hedderman, L. O. Neill, G. Chambers, H. J. Byrne, *Carbon* **42**, 1031 (2004).
- [19] S. Irle, H. Lischka, *J. Mol. Struct.* **364**, 15 (1996).
- [20] H. W. Offen, *J. Chem. Phys.* **44**, 699 (1966).
- [21] P. F. Jones, M. Nicol, *J. Chem. Phys.* **48**, 5440 (1968).
- [22] Z. A. Dreger, H. Lucas, Y. M. Gupta, *J. Phys. Chem.* **107**, 9268 (2003).
- [23] S-H. Lim, T. G. Bjorklund, C. J. Bardeen, *Chem. Phys. Lett.* **342**, 555 (2001).
- [24] I. Baltog, L. Mihut, M. Baibarac, N. Preda, T. Velula, S. Lefrant, *J. Optoelectron. Adv. Mater.* **7**(4), 2165 (2005).
- [25] L. Mihut, N. Preda, M. Baibarac, I. Baltog, S. Lefrant, J. Wery, *Mol. Cryst. Liq. Cryst.* **416**, 13 (2004).